

Analytical and Numerical Analysis of Load Gerotor Pumps

Lozica Ivanović¹⁾
Mirko Blagojević¹⁾
Goran Devedžić¹⁾
Yasmina Assoul²⁾

This paper deals with forces and moments that influence the gearing pair of the rotary trochoidal pump. The objective of this study was to analyze the impact of the pump chamber to load distribution in trochoidal pumps with fixed shaft axes. Problem of contact forces determination is a complex one because of the fact that load is transferred, at the same time, into several contact points. Besides that, there is the analysis of fluid pressure forces which act on the gear wheel tooth flanks and which depend on a large number of influential parameters. A simple physical model and an appropriate analytical method are applied. For the verification of the analytical method, as well as for computation of current moments and support reaction, the finite element method was used.

Key words: pumps, gerotor, gearing pair, gearing, contact load, load analysis, force analysis, finite element method

Introduction

GEOMETRY of the trochoids and their coupled envelopes is defined and analyzed in detail in [1-3]. Modifications of the trochoids and definitions of geometrical limitations are analyzed in [4-6]. A kinematic analysis of the trochoidal gearing in the gerotor is presented in papers [7, 8]. The application of the modern theory of gearing in the generation of cycloidal gearing is presented in [9-14]. The methodology for the selection of the optimal shape profile of teeth for lubrication pumps is described in paper [15].

This paper deals with the gearing of the trochoidal pump gearing pair where the outer gear has one more tooth than the inner one. The inner gear profile is described by peritrochoid equidistant while the profile of the outer gear is described by a circular arc with r_c radius. For trochoidal gearing, meshing of all teeth is obtained, at the same time, with theoretical profiles of gearing. This is the reason that general equations of profile point coordinates need to be established, so that they could be applied for all teeth. Towards derivation of coordinates equations for any P_i contact point, it was needed to generalize the geometric relations between the rotation angles of the trochoidal gearing couple elements. A kinematic pair model with the fixed gear shaft axes was adopted, whereby the drive shaft is connected to the inner gear. Further on, forces and moments that act on the gearing pair of the rotary trochoidal pump are discussed. A modified analytical method presented by Colbourne and Maiti in their papers [16, 17] is applied for the analysis of forces and moments. For the verification of the analytical method, as well as for the calculation of current moments and support reaction, the finite element method was used [18, 19].

Gearing geometry

Before the analysis of trochoidal profiles meshing, the applied coordinate systems and the geometric relations between the rotation angles in different coordinate systems will be presented. The basic geometric relations for the generation of peritrochoid, which is adopted for defining the basic profile at the observed gear pump, are shown in Fig.1. The center and the radius of movable (generative) circle are marked as O_a and r_a , respectively, while O_t and r_t denote those values for the stationary (main) circle. The eccentricity of the trochoid, marked as e , represents the distance between the two centers of the circle. The generative coordinate system $O_a x_i y_i$ is tied to the center of the movable circle. The generative D_i point is the point that describes the trochoid and is placed at the x_i axis at the d distance from the O_a center and represents the size of the radius of the trochoid. The reference line is determined by the line that connects O_t and O_a centers and that goes through the contact point of the two circles, that is, through the kinematic pole C . In order to represent the trochoidal profile in the analytical form, the coordinate system $O_t x_t y_t$ of the trochoid is introduced and its start is set up at the center of the stationary circle, while the abscissa goes through the starting contact point of the given kinematic circles. The coordinate system $O_a x_a y_a$ of the envelope is tied to the center of the movable circle. The stationary coordinate system $O_f x_f y_f$ is tied to the center of the kinematic circle of the trochoid, that is, $O_f = O_t$. All coordinate systems are of the right orientation. At the starting instant, the positive part of the x_t axis for the inner

¹⁾ Faculty of Mechanical Engineering, University of Kragujevac, Sestre Janjić 6, 34000 Kragujevac, SERBIA

²⁾ Faculty of Engineering, Université Saâd Dahleb Blida, ALGÉRIA

gear is tied to the tip of the starting tooth, while the positive part of the x_a axis for the outer gear concurs with the centerline of the hollow between the meshing teeth.

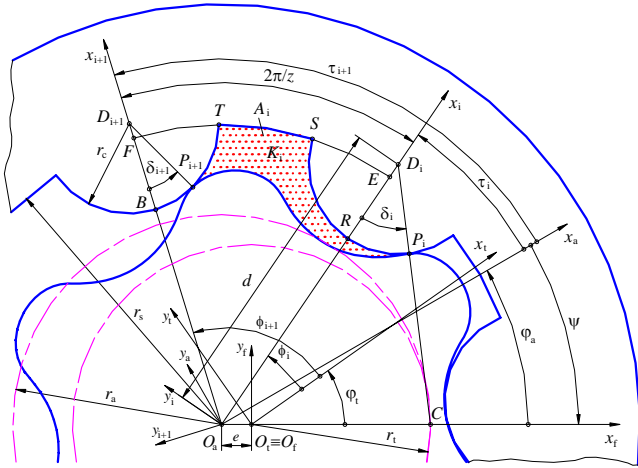


Figure 1. Schematic presentation of the gearing pair of the trochoidal pump and of the basic geometric variables for the P_i contact point and for the P_{i+1} contact point

The position vector of the P_i contact point in the coordinate system of the trochoid can be written in the form of the following matrix relation:

$$\mathbf{r}_{P_i}^{(t)} = \begin{bmatrix} e[\cos z\phi_i + \lambda z \cos \phi_i - c \cos(\phi_i + \delta_i)] \\ e[\sin z\phi_i + \lambda z \sin \phi_i - c \sin(\phi_i + \delta_i)] \\ 1 \end{bmatrix}. \quad (1)$$

In equation (1) λ is the trochoid coefficient as

$$\lambda = \frac{d}{ez}, \quad (2)$$

where c is the coefficient of the equidistant radius as

$$c = \frac{r_c}{e}, \quad (3)$$

ϕ_i is the angle between the x_i and x_a axes

$$\phi_i = \tau_i + \frac{\psi}{z-1}, \quad (4)$$

ψ is the angle between the x_a and x_f axes

τ_i is the angle between the x_i and x_a axes

$$\tau_i = \frac{\pi(2i-1)}{z} \quad (5)$$

and δ_i is the leaning angle as

$$\delta_i = \arctan \frac{\sin(\tau_i - \psi)}{\lambda - \cos(\tau_i - \psi)}. \quad (6)$$

In the coordinate system of the $O_a x_a y_a$ envelope, the position vector of the P_i contact point is given as in the equation:

$$\mathbf{r}_{P_i}^{(a)} = \mathbf{M}_{at} \mathbf{r}_{P_i}^{(t)} = \begin{bmatrix} e[z\lambda \cos \tau_i - c \cos(\tau_i + \delta_i)] \\ e[z\lambda \sin \tau_i - c \sin(\tau_i + \delta_i)] \\ 1 \end{bmatrix} \quad (7)$$

where \mathbf{M}_{at} is the transformation matrix from the trochoid

coordinate system into the envelope coordinate system as

$$\mathbf{M}_{at} = \begin{bmatrix} \cos \frac{\psi}{z-1} & \sin \frac{\psi}{z-1} & e \cos \psi \\ -\sin \frac{\psi}{z-1} & \cos \frac{\psi}{z-1} & e \sin \psi \\ 0 & 0 & 1 \end{bmatrix}. \quad (8)$$

By the application of the following matrix equation

$$\mathbf{r}_{P_i}^{(f)} = \mathbf{M}_{fa} \mathbf{r}_{P_i}^{(a)}, \quad (9)$$

where \mathbf{M}_{fa} is the transformation matrix from the envelope coordinate system into the stationary coordinate system as

$$\mathbf{M}_{fa} = \begin{bmatrix} \cos \psi & \sin \psi & -e \\ -\sin \psi & \cos \psi & 0 \\ 0 & 0 & 1 \end{bmatrix}, \quad (10)$$

an equation of the contact line of the meshing profiles is obtained as:

$$\mathbf{r}_{P_i}^{(f)} = \begin{bmatrix} e[z\lambda \cos(\tau_i - \psi) - 1 - c \cos(\tau_i - \psi + \delta_i)] \\ e[z\lambda \sin(\tau_i - \psi) - c \sin(\tau_i - \psi + \delta_i)] \\ 1 \end{bmatrix}. \quad (11)$$

After defining the gearing geometry of the gerotor pump gearing pair and after establishing a basic kinematic model, calculation of forces and moments, which act on the gears, is enabled.

Load analysis for trochoidal pumps with stationary shaft axes

Both analytical and numerical methods are applied within the scope of this paper, in order to solve problems in connection with load analysis for the trochoidal pumps with the stationary axes of shafts.

In the first part of the paper, the analytical method is presented for the computation of current moments and contact forces at trochoidal pumps with stationary shaft axes and when the drive shaft is tied to the inner gear. When the drive moment affects the inner gear it will rotate around its axis until achieving gear deformation of such a magnitude to create forces whose resulting moment around the center of the outer gear is equal to the moment of the fluid pressure force around that same point.

Fluid pressure force

During the calculation of the fluid pressure force the assumption was made that pressure change within chambers can be neglected, i.e. the pressure in all chambers of the same zone (the suction inlet or the pressure outlet chambers) is of a constant value, $p_{i(in)} = const$,

$p_{i(out)} = const$. In this case, the fluid pressure force which separates the suction inlet chambers from the pressure outlet chambers is a continuous force that can be represented by the equivalent concentrated pressure force \mathbf{F}_p , whose vector's direction coincides with the centerline of the line segment **AB** that connects two contact points at the separation borderline between the suction inlet chambers and the pressure outlet chambers zones, as shown in Fig.2. In accordance with this, the equivalent pressure force

in the pump can be expressed in a vector form such as:

$$\mathbf{F}_p^{(f)} = -\Delta p b \mathbf{k}_f \times \mathbf{AB}^{(f)}, \quad (12)$$

where Δp is the pressure drop at the pump and b is the gear width.

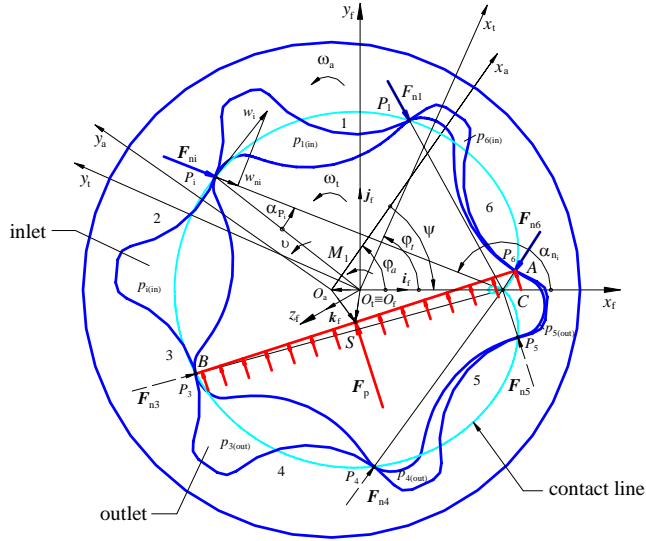


Figure 2. Fluid pressure force and contact forces that act on the inner gear at a random instant ($\varphi_a = 55^\circ$) [18]

The vector \mathbf{AB} that connects two contact points at the separation borderline between the suction inlet chambers and the pressure outlet chambers zones can be expressed as a difference between the position vectors for these points in a stationary coordinate system as:

$$\mathbf{AB}^{(f)} = \mathbf{r}_B^{(f)} - \mathbf{r}_A^{(f)} = \begin{bmatrix} x_B^{(f)} - x_A^{(f)} \\ y_B^{(f)} - y_A^{(f)} \\ 0 \end{bmatrix}. \quad (13)$$

When equation (13) is inserted into equation (12) the following resulting expression is obtained:

$$\mathbf{F}_p^{(f)} = -\Delta p b \begin{vmatrix} \mathbf{i}_f & \mathbf{j}_f & \mathbf{k}_f \\ 0 & 0 & 1 \\ x_B^{(f)} - x_A^{(f)} & y_B^{(f)} - y_A^{(f)} & 0 \end{vmatrix}. \quad (14)$$

The moment of the equivalent pressure force, in relation with the current center of the rotation C can be expressed in the following form of the vector multiplication equation:

$$\mathbf{M}_p^{(f)} = \mathbf{CS}^{(f)} \times \mathbf{F}_p^{(f)}, \quad (15)$$

where S is the central point of the vector \mathbf{AB} (Fig.2).

Based on the geometric relations shown in Fig.2, the following vector relations can be written as:

$$\mathbf{CS} = \frac{1}{2}(\mathbf{CA} + \mathbf{CB}). \quad (16)$$

By applying the rules of vector addition, the following expression is obtained:

$$\mathbf{CS}^{(f)} = \frac{1}{2} \left[(x_{CA}^{(f)} + x_{CB}^{(f)}) \mathbf{i}_f + (y_{CA}^{(f)} + y_{CB}^{(f)}) \mathbf{j}_f \right]. \quad (17)$$

Starting with equation (12), the equivalent pressure force can be expressed by the next form:

$$\mathbf{F}_p^{(f)} = \Delta p b \left[(y_{CB}^{(f)} - y_{CA}^{(f)}) \mathbf{i}_f - (x_{CB}^{(f)} - x_{CA}^{(f)}) \mathbf{j}_f \right]. \quad (18)$$

By putting equations (17) and (18) into (15), the equivalent pressure force moment in the pump can be expressed in the form of the following relation:

$$\mathbf{M}_p^{(f)} = \begin{vmatrix} \mathbf{i}_f & \mathbf{j}_f & \mathbf{k}_f \\ \frac{1}{2} [x_{CB}^{(f)} + x_{CA}^{(f)}] & \frac{1}{2} [y_{CB}^{(f)} + y_{CA}^{(f)}] & 0 \\ \Delta p b [y_{CB}^{(f)} - y_{CA}^{(f)}] & -\Delta p b [x_{CB}^{(f)} - x_{CA}^{(f)}] & 0 \end{vmatrix}, \quad (19)$$

which can be represented in the simpler form as:

$$\mathbf{M}_p^{(f)} = \frac{\Delta p b}{2} (|\mathbf{CA}|^2 - |\mathbf{CB}|^2) \mathbf{k}_f. \quad (20)$$

The resultant of all the contact forces that act on the inner gear is obtained as their vector sum:

$$\mathbf{F}_n = \sum_{i=1}^z \mathbf{F}_{ni} \quad (21)$$

whereby its vector endpoint coincides with the kinematic pole C .

After the realised procedure and with the application of the obtained expressions for calculating external load, the analysis of load distribution can be started. Two cases are distinguished as follows [17, 18, 19]:

1. case I, when the vector line of pressure force goes between the centers of the gears;
2. case II, when the vector line of pressure force does not go between the centers of the gears.

For both cases, a position exists for which the vector line of pressure force goes through the center O_a , which points to the moment when, theoretically, the contact forces do not exist, i.e. some teeth leave the contact and contact load is transferred to another teeth. Then, in case II, the moment of contact forces changes its sign.

Unlike with models with planetary movement, where fluid pressure force is balanced by the resultant of contact forces, the support reaction, denoted as \mathbf{F}_1 , is included in equilibrium equations for the model used in this paper. Unknown forces that act on the gear, including the support reaction, are determined from the conditions of equilibrium, for the two-dimensional system of forces, i.e. it is necessary for both the resultant force and the resultant moment to be equal to zero. For the observed pump model, the force equilibrium equation in a vector form can be written as:

$$\mathbf{F}_p + \mathbf{F}_n + \mathbf{F}_1 = 0. \quad (22)$$

Then, the moment of equilibrium equations can be written, in relation to the point O_t :

$$\mathbf{M}_{F_p(O_t)} + \mathbf{M}_{F_n(O_t)} + \mathbf{M}_1 = 0 \quad (23)$$

and in relation to the point O_a :

$$\mathbf{M}_{F_p(O_a)} + \mathbf{M}_{F_n(O_a)} = 0. \quad (24)$$

When the moments from the previous equations are expressed in a form of vector multiplication equations, the following expressions are obtained:

$$\mathbf{O}_t \mathbf{S} \times \mathbf{F}_p + \mathbf{O}_t \mathbf{C} \times \mathbf{F}_n + \mathbf{M}_1 = 0 \quad (25)$$

and

$$\mathbf{O}_a \mathbf{S} \times \mathbf{F}_p + \mathbf{O}_a \mathbf{C} \times \mathbf{F}_n = 0 \quad (26)$$

From equations (24) and (26), the moment of contact forces can be expressed as:

$$\mathbf{M}_{F_n(O_a)}^{(f)} = -\mathbf{M}_{F_p(O_a)}^{(f)} = -\mathbf{O}_a \mathbf{S}^{(f)} \times \mathbf{F}_p^{(f)}. \quad (27)$$

Based on the geometric relations shown in Fig.2, the following vector relation can be written:

$$\mathbf{O}_i \mathbf{S} = \frac{1}{2}(\mathbf{O}_i \mathbf{A} + \mathbf{O}_i \mathbf{B}), \quad (28)$$

That is,

$$\mathbf{O}_i \mathbf{S}^{(f)} = \frac{1}{2} \left[(x_A^{(f)} + x_B^{(f)}) \mathbf{i}_f + (y_A^{(f)} + y_B^{(f)}) \mathbf{j}_f \right]. \quad (29)$$

In a similar way, the following relations can be written:

$$\mathbf{O}_a \mathbf{S} = \mathbf{O}_i \mathbf{S} - \mathbf{O}_i \mathbf{O}_a, \quad (30)$$

$$\mathbf{O}_i \mathbf{O}_a^{(f)} = -e \mathbf{i}_f \quad (31)$$

and after their arrangement, the final expression is obtained as:

$$\mathbf{O}_a \mathbf{S}^{(f)} = \frac{1}{2} \left[(x_A^{(f)} + x_B^{(f)} + 2e) \mathbf{i}_f + (y_A^{(f)} + y_B^{(f)}) \mathbf{j}_f \right]. \quad (32)$$

By putting equations (14) and (32) into (27), the moment of equivalent contact force in relation to the point O_a , can be expressed in a form of the following vector relation:

$$\mathbf{M}_{F_n(O_a)}^{(f)} = \begin{vmatrix} \mathbf{i}_f & \mathbf{j}_f & \mathbf{k}_f \\ -\frac{1}{2} [x_A^{(f)} + x_B^{(f)} + 2e] & -\frac{1}{2} [y_A^{(f)} + y_B^{(f)}] & 0 \\ -\Delta pb [y_A^{(f)} - y_B^{(f)}] & \Delta pb [x_A^{(f)} - x_B^{(f)}] & 0 \end{vmatrix} \quad (33)$$

or in a scalar form as:

$$\mathbf{M}_{F_n(O_a)}^{(f)} = \frac{\Delta pb}{2} \left\{ [r_B^{(f)}]^2 - [r_A^{(f)}]^2 + 2e [x_B^{(f)} - x_A^{(f)}] \right\}. \quad (34)$$

The moment of equivalent contact force in relation to the point O_i , can be written in a form of the following vector relation:

$$\mathbf{M}_{F_p(O_i)}^{(f)} = \mathbf{O}_i \mathbf{S}^{(f)} \times \mathbf{F}_p^{(f)} \quad (35)$$

which, by putting equations (29) and (14) in it, results in the following form:

$$\mathbf{M}_{F_p(O_i)}^{(f)} = \begin{vmatrix} \mathbf{i}_f & \mathbf{j}_f & \mathbf{k}_f \\ \frac{1}{2} [x_A^{(f)} + x_B^{(f)}] & \frac{1}{2} [y_A^{(f)} + y_B^{(f)}] & 0 \\ -\Delta pb [y_A^{(f)} - y_B^{(f)}] & \Delta pb [x_A^{(f)} - x_B^{(f)}] & 0 \end{vmatrix} \quad (36)$$

The equation can be expressed in a scalar form as:

$$\mathbf{M}_{F_p(O_i)}^{(f)} = \frac{\Delta pb}{2} \left\{ [r_A^{(f)}]^2 - [r_B^{(f)}]^2 \right\}. \quad (37)$$

In equation (22), only the vector of the fluid pressure force, \mathbf{F}_p , is completely defined. Because of that, it is suitable for further calculation to write equation (23) in a scalar form as:

$$M_1 = -M_{F_p(O_i)} + M_{F_p(O_a)} \frac{z-1}{z}, \quad (38)$$

and then the moment of equivalent contact force can be determined, in relation to the center of the inner gear, O_i , which is necessary for the calculation of the contact forces.

Contact forces

During the gear motion, total normal load is transferred by synchronous teeth meshing of the gearing pair. The influence of the normal force F_{ni} on the meshing teeth provokes the appearance of the local deformation of the tooth and shifting of the contact point of w_{ni} magnitude, in direction of the force action. The consequence of the deformation is the angle of the displacement υ and based on Fig.2, the relations can be established between them as follows:

$$w_{ni} = r_{P_i}^{(f)} \upsilon \sin \alpha_{P_i}, \quad (42)$$

with an assumption that the elementary angle of the displacement υ is equal for all contact points [20]. In equation (42), α_{P_i} is the angle between the direction that connects the center of the inner gear, O_i with the contact point P_i and of the vector line of the normal force F_{ni} .

The normal force is proportional to the deformation in the normal direction as:

$$F_{ni} = k w_{ni}, \quad (43)$$

where k is gear rigidity and is considered to be a constant. Based on the geometric relations that apply to the triangle $O_i P_i C$ according to Fig.2, the following can be stated:

$$r_{P_i}^{(f)} = e(z-1) \frac{\sin \alpha_{ni}}{\sin \alpha_{P_i}} \quad (44)$$

where α_{ni} is the angle between the x_f axis and the \mathbf{CP}_i vector, as given in Fig.2.

For the determination of the α_{ni} angle, it is necessary to define the $\mathbf{CP}_i^{(f)}$ vector. The position vector of the point C in the $O_f x_f y_f z_f$ coordinative system can be written in the following form:

$$\mathbf{r}_C^{(f)} = e(z-1) \mathbf{i}_f \quad (45)$$

Going from the geometric relation given in Fig.2 and equations (11) and (45), the $\mathbf{CP}_i^{(f)}$ vector can be expressed as:

$$\mathbf{CP}_i^{(f)} = \mathbf{r}_{P_i}^{(f)} - \mathbf{r}_C^{(f)} \quad (46)$$

$$\mathbf{CP}_i^{(f)} = \begin{bmatrix} e [z \lambda \cos(\tau_i - \psi) - z - c \cos(\tau_i - \psi + \delta_i)] \\ e [z \lambda \sin(\tau_i - \psi) - c \sin(\tau_i - \psi + \delta_i)] \\ 1 \end{bmatrix} \quad (47)$$

and the angle α_{ni} as:

$$\alpha_{ni} = \arctan \frac{y_{\mathbf{CP}_i}^{(f)}}{x_{\mathbf{CP}_i}^{(f)}}. \quad (48)$$

If the deformation w_{ni} in the contact point P_i is larger than zero, it means that contact is realised in that point. However, if the deformation w_{ni} in the contact point P_i is negative or equal to zero, contact is not realised and those contact points do not participate in load distribution. A total moment of normal forces is equal to the sum of the moments of normal forces for individual teeth pairs, around the gear center as:

$$M_{F_n(O_t)} = \sum_{i=p}^q M_{F_{ni}(O_t)} = k_v \sum_{i=p}^q e^2 (z-1)^2 \sin^2 \alpha_{ni} \quad (49)$$

where p and q are ordinal numbers of the starting and the final tooth of the outer gear, which transfer load and k_v is an introduced constant equal to $k_v = k_v$. The constant k_v , whose value is necessary for the calculation of the contact forces, is obtained by the iterative procedure of solving equation (49) with the application of the following condition:

$$|M_{F_n(O_t)}| = \frac{z-1}{z} |M_{F_p(O_a)}|. \quad (50)$$

After the identification procedure of the teeth pairs that transfer load and contact forces calculation, an appropriate contact stress calculation is realised by using methods presented within references [16, 17]. A graphical representation of the analytical calculation of torque moments is given in Fig.3 and of contact forces in Fig.4.

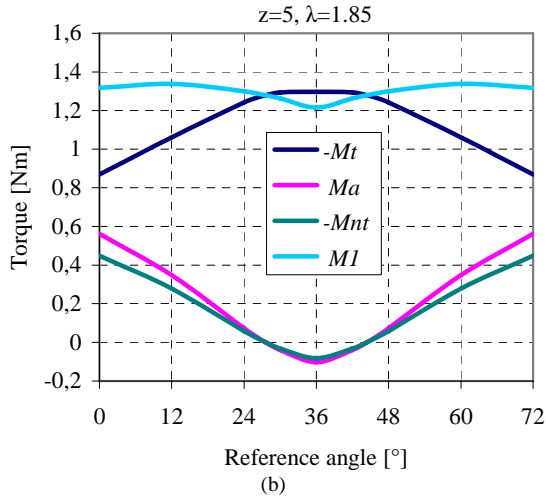


Figure 3. Results of the analytical calculation of the torque: (a) $z=6$ and (b) $z=5$

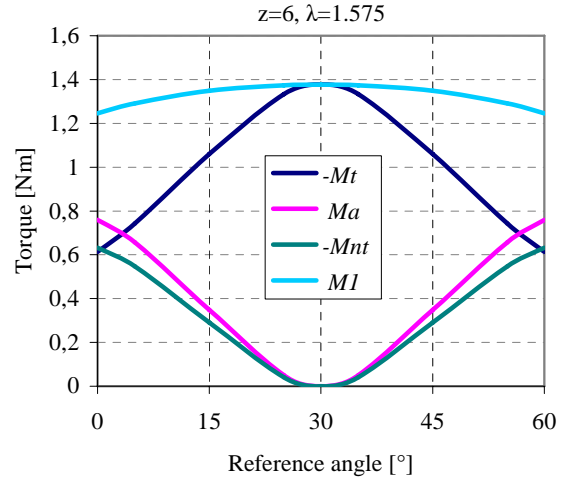
In order to illustrate the proposed procedures for the analysis of load trochoidal gear pairs as well as the comparative analysis of the results, two gear sets are selected, with their geometrical parameters given in Table 1. Other parameters are: $e=3.56$ mm, $b=16.46$ mm, $r_s=26.94$ mm, $\Delta p=0.6$ MPa, $\rho_f=900$ kg/m³, $n_t=1500$ rpm, $\omega_t = 2\pi n_t = 50\pi s^{-1}$.

Table 1: Geometrical parameters for the two gear set

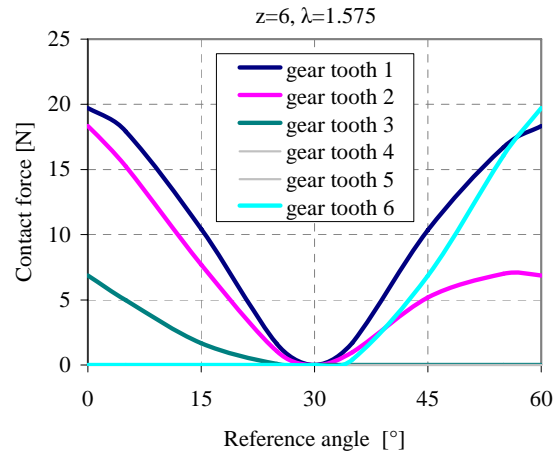
Parameters	z	λ	c
Gear set I	5	1.85	3.75
Gear set II	6	1.575	3.95

Other parameters are: $e=3.56$ mm, $b=16.46$ mm, $r_s=26.94$ mm, $\Delta p=0.6$ MPa, $\rho_f=900$ kg/m³, $n_t=1500$ rpm, $\omega_t = 2\pi n_t = 50\pi s^{-1}$.

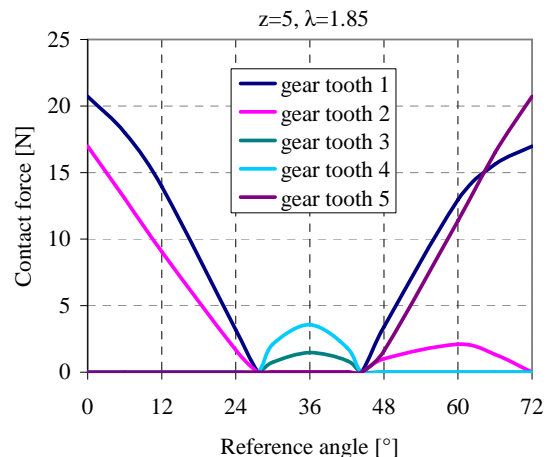
The results are presented in the function of the reference angle φ_a , for a period corresponding to the phase difference between two adjacent chambers, ie. $\varphi_a=2\pi/z$, where the calculation repeated for nine angular positions.



(a)



(a)



(b)

Figure 4: Results of the analytical calculation of the contact forces: (a) $z=6$ and (b) $z=5$

After the comparison of charts for various models of pumps, it can be concluded that the model with an odd number of teeth ($z = 5$) has a different character torque ripple from the model with even numbers of teeth, and the different distributions of the contact force. This is the implication of changing the sign of the contact force

moment during one phase of the work process. The highest values of the contact force are realized in the initial stages of the working process and they are increased in the pump with an odd number of chambers. It can be seen in Fig.4, where the teeth denoted with 4 and 5 do not make contact during the consideration phase.

Analysis of forces and moments by the application of the finite elements method

The load simulation for the trochoidal pump gears by the application of the CATIA software module for structural analysis is presented in this part of the paper. In order to realize the structural analysis, it is necessary to follow a certain procedure [18], which will be described in the following text.

Geometric model

A basic model used in the structural analysis corresponds to the inner cylindrical gear of the trochoidal pump. The geometric model is created within the PART module of the CATIA software package. It starts from the geometric shape of the profile of the cylindrical gear teeth based on the analytical-kinematic model [18], and by running the built computer program. The main CAD model of the unloaded gear contains 20 line segments.

Grid generating

During the first phase of the numerical model preparation, a three-dimensional tetrahedral grid of variable fineness is generated. A part of the grid around the contact force line is with discrete elements of the biggest fineness (0.75 mm element side length) and the rest is done with an element size of 1.5 mm. The gear shown in Fig.5 is modeled with 6779 nodes and 29260 finite elements, and the gear in Fig.6 is modeled with 6546 nodes and 27861 finite elements.

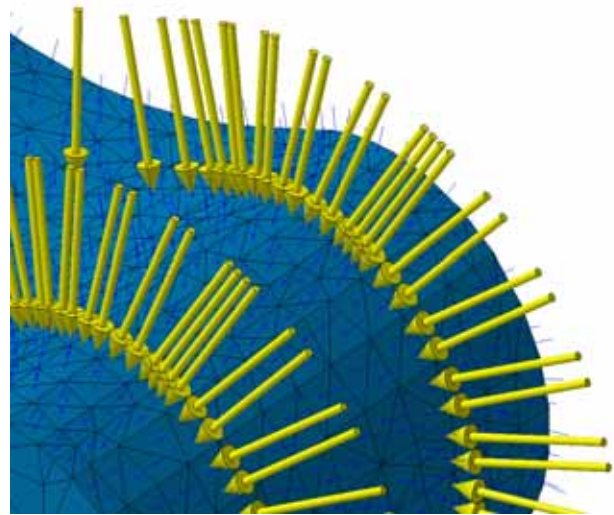
Boundary conditions of the numerical model

The boundary conditions are defined in accordance with the theoretical analysis of gears. The motion limit is set up on the surface that lies on the drive shaft and here all types of motion are forbidden such as: radial, axial and all rotations. In order to obtain the results, the torque moment and the support reaction force as well as the sensor in the gear section plane are defined.

Mechanical loads in the numerical model

During pre-processing, it is necessary to enter values for the forces that react with the gear, therefore defining all necessary parameters for processing, i.e. for the structural analysis by the finite elements method. For structure load, the relative pressure at the suction inlet and at the pressure outlet side is set up as well as the contact forces. The assumption is also made that the normal force F_{ni} is evenly distributed along the current line of the teeth flanks contact. By this, a computation model is completely described and statically determined.

The fluid pressure force is simulated by concentrated forces which act perpendicularly to the finite elements surfaces, which is illustrated in Fig.5. The presentation of the input forces for the load state with the angular position $\varphi_a=25^\circ$ is given in Fig.6, and for $\varphi_a=24^\circ$ in Fig.7.



Slika 5. Detail of the visualization of the discrete load gear

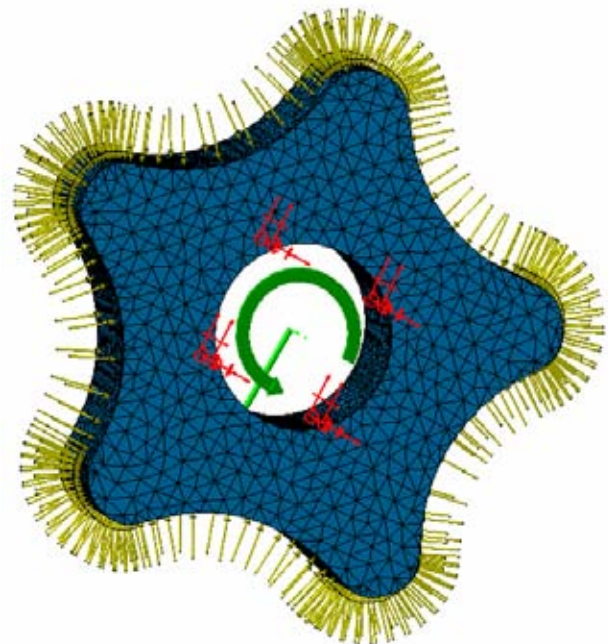


Figure 6. Model of the discrete gear simulation with forces defined and the results of visualization, $z=6$

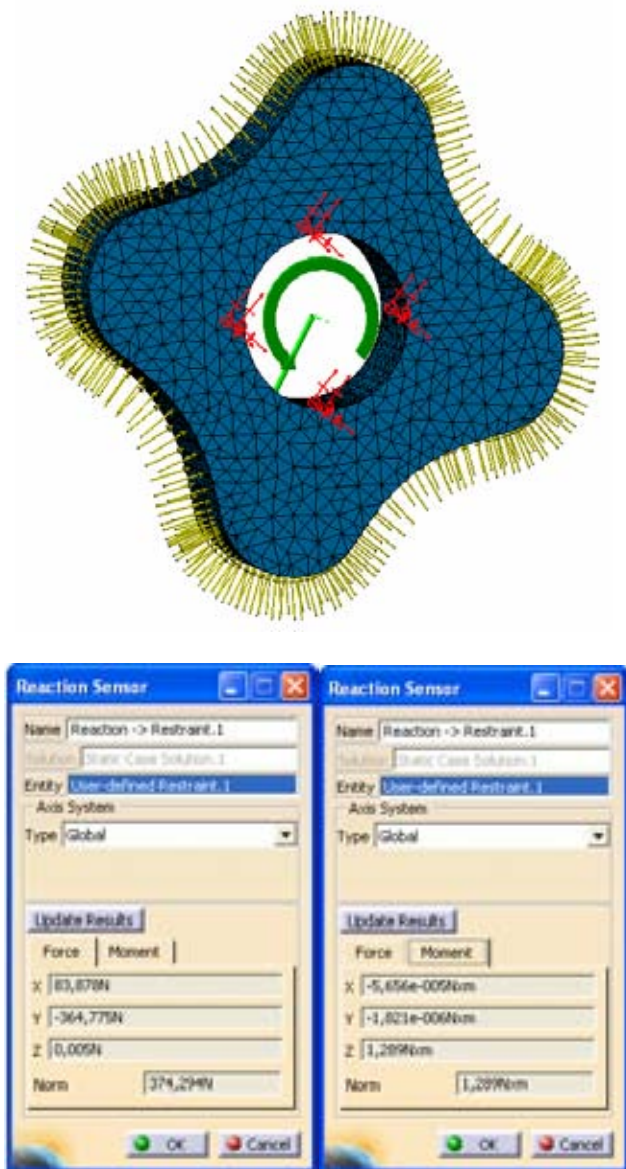


Figure 7. Model of the discrete gear simulation with forces defined and the results of visualization, $z=5$

Within the scope of static investigations, two separate computations are made:

1. only fluid pressure is set up as a structure load in the first case,
2. fluid pressure and contact forces are set up as a structure load in the second case.

The output results for the first case are the fluid pressure force and the moment which is equivalent to the contact forces moment. The obtained results are used for the analytical determination of contact forces. After the calculation of forces, the input of load to the model is done and then the calculation is realised with the drive moment and the support reaction force as output results. The second case is related to the real system, while the first case is comparatively important and issues data necessary for the load simulation in the second case. The output results are support reaction force and the drive moment as shown in Fig.7. The direct readout of the values of their projections on global coordinative system axes is enabled as well as the readout of the resulting algebraic values that has been used for the diagram drawing.

Graphical presentation and the analysis of computational results

It was necessary to repeat the procedure of the structural analysis several times for each chosen gear model, in order to realize the numerical computation. The number of repeating was nine for the computation model, i.e. eighteen for both calculations. The analysis was done for different angular positions starting from $\varphi_a=0$ until the final position that corresponds to the starting position of the following tooth, i.e. $\varphi_a=2\pi/z$ (Table 2).

Table 2: Angle positions of the gears for the load calculation

Positions	φ_a [°]	
	$z=6$	$z=5$
	0	0
	5	12
	15	24
	25	27,6155
	30	36
	35	44,3845
	45	48
	55	60
	60	72

The comparative values of the drive moment obtained by the analytical and the numerical method are shown in Fig.8. A very slight deviation of values indicates that the previously mentioned approximation, where the continuous force is represented by the equivalent concentrated pressure force, can be used for analytical calculations of load distribution at trochoidal pumps.

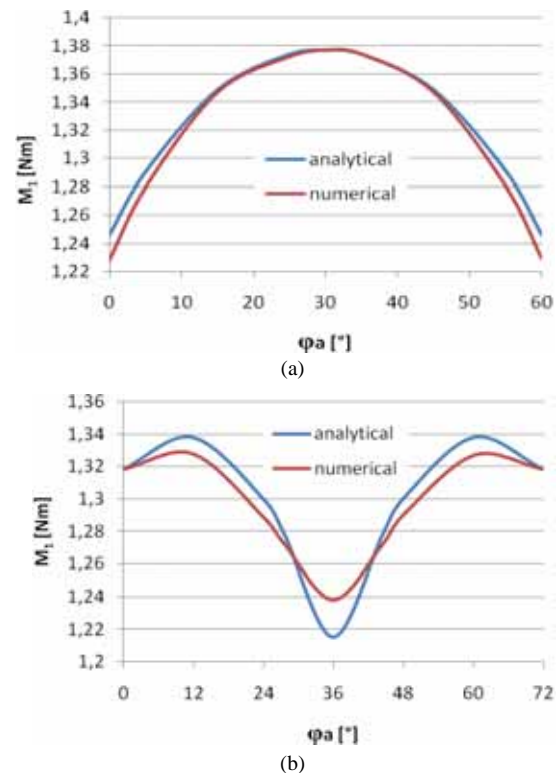


Figure 8. Results of the analytical and numerical calculations: (a) $z=6$ and (b) $z=5$

The comparative values of the fluid pressure force obtained by the analytical and the numerical methods for individual angular positions are shown in Fig.9.

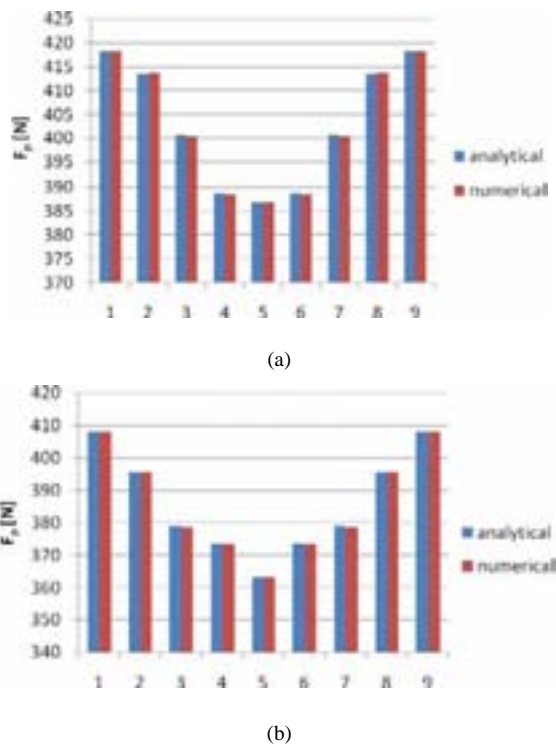


Figure 9. Results of the analytical and the numerical computations of the fluid pressure force: (a) $z=6$ and (b) $z=5$

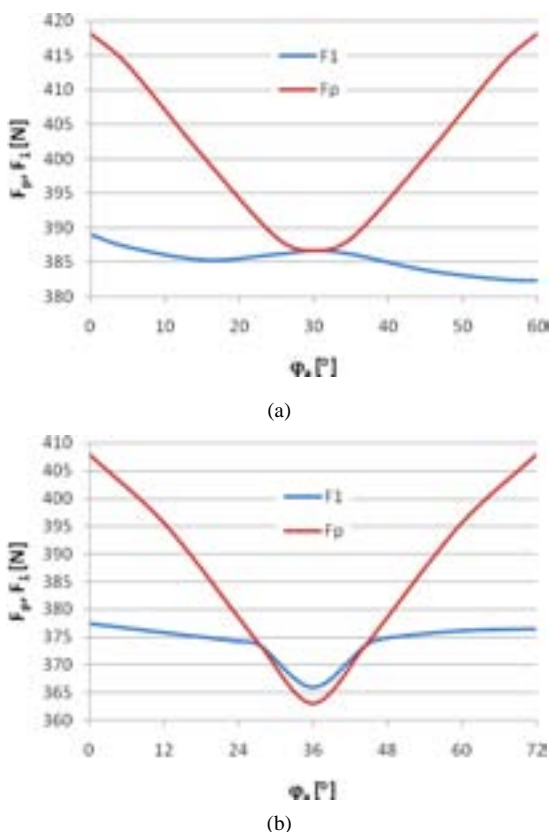


Figure 10. Charts of the numerical calculations as results of the fluid pressure force and the support reaction: (a) $z=6$ and (b) $z=5$

The dependence of the fluid pressure force F_p and the support reaction force F_1 on the reference rotation angle, for one phase of the pump working process, for both gear sets, is shown on the charts in Fig.10. These charts provide information on the domain of the force equivalent to the contact forces resultant as well as information about the

angular position where the interchange of load between the adjacent teeth occurs.

Conclusions

On the basis of the derived results, it can be concluded that the pumps with the same kinematic scheme, but with a different number of teeth, can have different static load models. Using the analytical method, the identification of teeth contact during one phase of the working process pumps is performed as well as the calculation of the contact force and the working moments. The highest values of the contact force are realized in the initial stages of the working process. They are also higher in the pump with an odd number of chambers. The values of the fluid pressure force F_p and the drive moment M_1 , obtained by numerical computation, are only slightly different from their analytical results. Both analytical and numerical method give satisfactory results necessary in analysing the influence of the variation of input parameters on the magnitude of contact forces.

Further research will be focused on the analysis of contact stress changes at gerotor pumps and the development of a model to identify the optimal geometric parameters of trochoidal gearing, towards the reducing of maximum contact stress.

References

- [1] ANSDALE,R.F., LOCKLEY,D.J.: *The Wankel RC Engine*, Iliffe Books Ltd., London, 1970, ISBN 0 592 00625 5.
- [2] COLBOURNE,J.R.: *The Geometry of Trochoid Envelopes and Their Application in Rotary Pumps*, Mechanism and Machine Theory 1974, 9, pp.421-435
- [3] SHUNG,J.B., PENNOCK,G.R.: *Geometry for Trochoidal-Type Machines With Conjugate Envelopes*, Mechanism and Machine Theory, 1994, Vol.29, No.1, pp.25-42.
- [4] ROBINSON,F.J., LYON,J.R.: *An Analysis of Epitrochoidal Profiles With Constant difference Modification Suitable for Rotary Expanders and Pumps*, Journal of Engineering for Industry, Trans. ASME, 1976, Vol.98, pp.161-165.
- [5] MAITI,R., SINHA,G.L.: *Limits on modification of epitrochoid used in rotary piston machines and the effects of modification on geometric volume displacement and ripple*, Ingenieur-Archiv, 1990, Vol.60, pp.183-194.
- [6] MAITI,R., SINHA,G.L.: *Kinematics of active contact in modified epitrochoid generated rotary piston machines*, Mechanism and Machine Theory, 1988, Vol.23, No.1, pp.39-45.
- [7] BEARD,J.E., YANNITELL,D.W., PENNOCK,G.R.: *The effects of the generating pin size and placement on the curvature and displacement of epitrochoidal gerotors*, Mechanism and Machine Theory, 1992, Vol.27, No.4, pp.373-389.
- [8] IVANOVIĆ,L., JOSIFOVIĆ,D.: *Specific Sliding of Trochoidal Gearing Profile in the Gerotor Pumps*, FME Transactions, 2006, Vol. 34, No. 3, pp. 121-127.
- [9] Litvin, F. L., Feng, P.: *Computerized design and generation of cycloidal gearings*, Mechanism and Machine Theory, 1996, Vol.31, No.7, pp.891-911.
- [10] MIMMI,G., PENNACCHI,P.: *Non-undercutting conditions in internal gears*, Mechanism and Machine Theory, 2000, Vol.35, pp.477-490.
- [11] MANCÒ,G., MANCÒ,S., RUNDO,M., NERVEGNA,N.: *Computerized generation of novel gearings for internal combustion engines lubricating pumps*, The International Journal of Fluid Power, 2000, Vol.1, No.1, pp.49-58.
- [12] VECCHIATO,D., DEMENEGO,A., ARGYRIS,J., LITVIN,F.L.: *Geometry of a cycloidal pump*, Computer methods in applied mechanics and engineering, 2001, Vol.190, pp.2309-2330.
- [13] DEMENEGO,A., VECCHIATO,D., LITVIN,F.L., NERVEGNA,N., MANCÒ,S.: *Design and simulation of meshing of a cycloidal pump*, Mechanism and Machine Theory, 2002, Vol.37, pp.311-332.

- [14] BLAGOJEVIĆ,M., NIKOLIĆ,V., MARJANOVIĆ,N., VELJOVIĆ,Lj.: *Analysis of Cycloid Drive's Dynamic Behavior*, Scientific Technical Review, 2009, Vol.LIX, No.1, pp.52-56.
- [15] IVANOVIĆ,L., JOSIFOVIĆ,D.: *Methodology for selection of the optimal trochoidal gear tooth profile at the lubricating pumps*, International Journal for Vehicle Mechanics, Engines and Transportation Systems, December 2008, Vol.34, No.4, pp.35-44.
- [16] COLBOURNE,J.R.: *Reduction of the Contact Stress in Internal Gear Pumps*, Journal of Engineering for Industry, Trans. ASME, Nov. 1976, Vol.98, No.4, pp.1296-1300.
- [17] MATTL,R.: *Active contact stresses at epitrochoid generated rotor-stator set of fixed axis or equivalent system ROPIMA type hydrostatic units*, Journal of Engineering for Industry, 1991, Vol.113, pp.465-473.
- [18] IVANOVIĆ,L.: *Identification of the Optimal Shape of Trochoid Gear Profile of Rotational Pump Elements*, PhD dissertation, The Faculty of Mechanical Engineering in Kragujevac, Kragujevac, 2007.
- [19] IVANOVIĆ,L., DEVEDŽIĆ,G., MIRIĆ,N., ČUKOVIĆ,S.: *Analysis of forces and moments in the gerotor pumps*, Proc. Instn Mech. Engrs, Part C: J. Mechanical Engineering Science (in press)
- [20] HLEBANJA,J. AND POBERAJ,I.: *Planetary transmissions with cycloid gearing for high transmission ratio*, In Proceedings of the First Yugoslav Conference of Machines and Mechanisms, Zagreb, Croatia, 1975, pp.113-136 (in Slovenian)

Received: 12.02.2010.

Analička i numerička analiza opterećenja gerotorskih pumpi

U ovom radu se razmatraju sile i momenti koji deluju na zupčasti par gerotorske pumpe. Cilj ovog rada je analiza uticaja broja komora pumpe na raspodelu opterećenja trohoidnih pumpi sa nepokretnim osama vratila. Problem određivanja kontaktnih sila je kompleksan s obzirom na to da se kod pumpi sa trohoidnim ozubljenjem opterećenje prenosi istovremeno u više tačaka dodira. Osim toga, razmatraju se sile pritiska fluida koje deluju na bokove zubaca zupčanika, a koje zavise od velikog broja uticajnih parametara. Iz tih razloga, primenjen je jednostavan fizički model i odgovarajuća analitička metoda. U ovom modelu kontinualna sila pritiska se aproksimira koncentrisanom silom čija je napadna tačka u središtu linije razdvajanja usisne i potisne zone. Za verifikaciju analitičke metode, kao i za proračun trenutnih momenata i reakcije oslonca primenjena je metoda konačnih elemenata.

Ključne reči: pumpe, gerotor, zupčasti par, ozubljenje, kontaktno opterećenje, analiza opterećenja, analiza sila, metoda konačnih elemenata.

Аналитический и цифровой анализ нагрузки героторных насосов

В настоящей работе рассматриваются силы и моменты действующие на зубчатую пару героторного насоса. Целью этой работы является анализ влияния числа камер насоса на распределение нагрузки трохойдальных насосов с неподвижными осами вала. Проблема определения контактных сил очень сложная, учитывая то, что у насосов с трохойдальной насечкой нагрузка передаётся одновременно в большое число точек соприкосновения. Кроме того, здесь рассматриваются силы напряжения жидкостей действующие на боки зубцов у зубчатого колеса, которые зависят от большого числа влияющих параметров. Из-за этих причин, применена простая физическая модель и соответствующий аналитический метод. В этой модели непрерывная сила давления приблизительно определяется силой сосредоточения, чья точка приложения находится в фокусе линии отрыва зоны всасывания от зоны тяги. Для контроля и официального подтверждения аналитического метода, а в том числе и расчёта мгновенных моментов и опорной реакции здесь применён метод конечных элементов.

Ключевые слова: Насосы, геротор, зубчатая пара, насечка, контактная нагрузка, анализ нагрузки, анализ сил, метод конечных элементов.

Analyse analytique et numérique de la charge chez les pompes gérotors

Les forces et les moments qui agissent sur le pair denté des pompes gérotors sont considérés dans ce papier. Le but de ce travail est l'analyse de l'influence du nombre des chambres de la pompe sur la distribution de la charge chez les pompes trochoïdales aux axes fixes des arbres. Le problème de la détermination des forces de contact est complexe étant donné que la charge est transférée simultanément à plusieurs points de contact chez les pompes aux dentures trochoïdales. En outre, on considère les forces de pression du fluide qui agissent aux flancs des dents de l'engrenage et ces forces dépendent de nombreux paramètres importants. Pour cette raison, on a utilisé un modèle physique simple ainsi qu'une méthode analytique appropriées. Chez ce modèle la force continue de pression se rapproche à la force concentrée dont le point d'attaque se trouve au centre de la ligne de démarcation de la zone de succion et de celle de la poussée. Pour vérifier la méthode analytique, ainsi que la computation des moments courants et la réaction du support, on a employé la méthode des éléments finis.

Mots clés: pompe, gérotor, pair de dents, denture, charge de contact, analyse de la charge, analyse des forces, méthode des éléments finis.